



HAL
open science

Catalyst-Free Epoxy Vitrimers Based on Transesterification Internally Activated by an α -CF 3 Group

Dimitri Berne, Florian Cuminet, Sébastien Lemouzy, Christine Joly-Duhamel,
Rinaldo Poli, Sylvain Caillol, Eric Leclerc, Vincent Ladmiral

► **To cite this version:**

Dimitri Berne, Florian Cuminet, Sébastien Lemouzy, Christine Joly-Duhamel, Rinaldo Poli, et al..
Catalyst-Free Epoxy Vitrimers Based on Transesterification Internally Activated by an α -CF 3 Group.
Macromolecules, 2022, 55, pp.1669-1679. 10.1021/acs.macromol.1c02538 . hal-03583794

HAL Id: hal-03583794

<https://hal.science/hal-03583794v1>

Submitted on 22 Feb 2022

HAL is a multi-disciplinary open access archive for the deposit and dissemination of scientific research documents, whether they are published or not. The documents may come from teaching and research institutions in France or abroad, or from public or private research centers.

L'archive ouverte pluridisciplinaire **HAL**, est destinée au dépôt et à la diffusion de documents scientifiques de niveau recherche, publiés ou non, émanant des établissements d'enseignement et de recherche français ou étrangers, des laboratoires publics ou privés.

Catalyst-free epoxy vitrimers based on transesterification internally activated by an α -CF₃ group

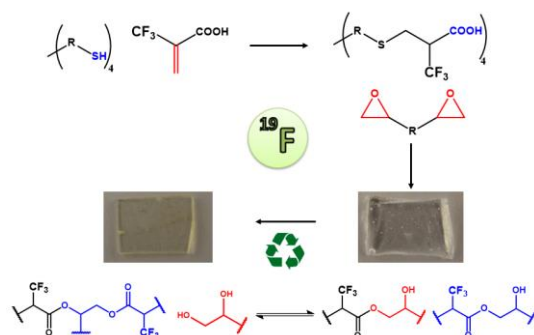
Dimitri Berne^a, Florian Cuminet^a, Sébastien Lemouzy^a, Christine Joly-Duhamel^a, Rinaldo Poli^{b,c}, Sylvain Caillol^a, Eric Leclerc^a, Vincent Ladmiral^{a*}

^a ICGM, Univ Montpellier, CNRS, ENSCM, Montpellier, 34293, France

^b CNRS, LCC (Laboratoire de Chimie de Coordination), Université de Toulouse, UPS, INPT, 205 Route de Narbonne, BP 44099, F-31077, Toulouse Cedex 4, France

^c Institut Universitaire de France, 1 rue Descartes, 75231 Paris Cedex 05, France

CAN, vitrimer, catalyst-free vitrimer, internal catalysis, neighboring group participation, epoxy chemistry, DFT



ABSTRACT: Vitrimers are polymer networks in which associative exchange reactions can take place under specific conditions, thus conferring reprocessability to the insoluble materials. Recently, catalyst-free vitrimers have emerged as a new generation of vitrimers able to overcome potential leaching, ageing and sintering issues of catalysts and to ensure the preservation of the vitrimer properties after numerous reshaping processes. Here, a catalyst-free epoxy vitrimer featuring α -CF₃-substituted ester functions is reported. First, a new tetra-acid precursor was synthesized via a catalyst-free thia-Michael addition. A catalyst-free ring-opening polymerization was then performed on two different di-epoxy monomers (DGEBA and BDGE) to obtain polymer networks composed of ester linkages. Curing was evaluated by rheology, DSC and FTIR monitoring of the polymerization kinetics. A gel content of over 70 % was measured after 24 h in THF. Finally, the accelerating effect of the α -CF₃ group on the transesterification reactions was highlighted by stress relaxation experiments and analyzed computationally on a molecular model system. Reprocessability tests were carried out at 150 °C for 2 h. The mechanical and thermal properties of the reshaped materials were similar to those of the initial ones. This study demonstrates the potential of fluorinated groups as powerful internal activators for transesterification vitrimers.

INTRODUCTION

Thermosets are a class of polymers composed of a three-dimensional network of polymer chains linked by covalent bonds. Such topology gives solid networks with insolubility properties and therefore this class of polymers has been used for structure, coatings, adhesives, electronics and composites applications. However, thermosets cannot be reshaped nor recycled as their composing bonds are irreversible. In contrast, thermoplastics that are composed of entangled linear polymer chains can be reprocessed above their glass transition temperature. Unfortunately, thermoplastics cannot be used for applications involving aggressive environments such as high temperature or solvents. Following the idea to couple the mechanical and chemical

resistance of thermosets with the reprocessability of thermoplastics, methods were developed to synthesize polymer networks containing reversible or exchangeable links.

Covalent adaptable networks (CANs) possess covalent bonds able to undergo exchange reactions, under photo- or thermal-activation for example, allowing the network structure to rearrange.¹⁻³ Dissociative and associative mechanisms have been developed to allow this structural rearrangement. Examples of dissociative chemistry are Diels-Alder addition,⁴⁻⁷ TAD chemistry,^{8,9} thia-Michael addition,^{10,11} oxime transcarbamoylation,¹² or alkoxyamine bond dissociation.¹³ In dissociative CANs, a bond has to be broken before a new cross-link can be formed, which in-

duces a temporary decrease of the cross-link density, particularly at high temperature where the bond lifetime becomes shorter. Vitrimers, introduced by L. Leibler in 2011,¹⁴ are a class of CANs in which the exchange reaction proceeds *via* an associative mechanism, keeping the cross-link content in the material constant at any reprocessing temperatures. A fastly expanding range of exchange reactions such as transesterification,¹⁴ transamination,^{15,16} transcarbamoylation,¹⁷ transimination,¹⁸ transalkylation,¹⁹ transacetalation,²⁰ boronate metathesis,²¹ transamidation,²² and acid exchange^{23,24} have been used in vitrimer chemistry.

Networks formed from epoxy–acid and epoxy–anhydride curing systems and based on dynamic transesterification are the most studied class of vitrimers.^{25–27} A wide range of epoxy monomers and hardeners is described in the literature^{28,29} and currently used in automotive, health and energy applications. Transesterification exchange reactions occur between ester bonds and hydroxyl groups available in the network. Catalysts are generally required to trigger these transesterification reactions and enable reshaping. The catalyst concentration has a direct impact on the bond-exchange reaction rate which, in turn affects the relaxation and reprocessing properties.^{30,31} Indeed, Leibler *et al.* demonstrated that an epoxy/anhydride material (with a final ester/hydroxyl group ratio of 1) containing only 0.1% of a Zn catalyst did not have vitrimer properties in contrast to analogous materials containing 5 or 10 mol % of catalyst.³⁰ Nevertheless, the use of external catalysts has several drawbacks. Indeed, organic salts^{32,33} and strong bases,³⁴ used as catalysts in epoxy vitrimers, are usually toxic and corrosive, and may leach from the materials or undergo ageing, thus reducing the panel of possible applications for these materials.³⁵ Moreover, the catalyst solubility in polymer may be limited, leading to heterogeneous systems when using high loadings. To reshape these catalyst-containing transesterification vitrimers, high temperatures (over 150°C) are often needed. At such elevated temperatures the catalysts may also accelerate the thermal degradation of the network,³⁶ with potential loss of mechanical and thermal properties after multiple reprocessings.³⁷

Catalyst-free vitrimers have been developed to address these catalyst-induced negative effects. As described by the team of F. Du Prez,³⁸ two mechanisms can be distinguished to explain the additive-free activation of exchange reactions. Recently, our group highlighted the existing examples of neighbouring group participation (NGP) and internal catalysis applied to vitrimers, but also the literature describing such effect at the molecular level and that could be implemented in materials.³⁹ First, NGP is associated to substituent effects that stabilize the transition state by bonding to the reaction centre. Additional hydroxyl functions^{40,41} or carboxylic acid^{42,43} in epoxy networks act as participating group by facilitating dynamic exchange reactions via H-bonding activation of the carbonyl groups. This NGP effect was already potentially at play in Leibler's first

vitrimers due to the presence of β -hydroxy ester links.¹⁴ Amines^{44,45} and benzenesulfonic acid⁴⁶ substituents may also act as participating group through the formation of cyclic intermediates. The second mechanism, often improperly called internal catalysis, corresponds to the rate-enhancing effect caused by electronic interactions. A set of β -activated ester-based vitrimers have been reported to be reprocessed at 150 °C under catalyst-free conditions. Diethylmalonate was used to crosslink a linear polyester, resulting in ester functions activated in this case by the electron-withdrawing effect of the $-C=O$ group placed in β -position.⁴⁷ Nevertheless, the stabilization by formation of a cyclic intermediate could also explain the rate-enhancing effect in this case.

With the objective of demonstrating the potential of electronically activated vitrimers, networks incorporating α -CF₃ esters and β -hydroxyl functions have been prepared. Here, we report catalyst-free epoxy vitrimers prepared from the reaction of a α -CF₃ tetra-acid (TTA) obtained by thia-Michael addition onto 2-(trifluoromethyl)acrylic acid (MAF) and a di-epoxy monomer: bisphenol A diglycidyl ether (DGEBA) or 1,4-butanediol diglycidyl ether (BDGE). The polyaddition reaction was evaluated by DSC and FTIR kinetic analyses and by rheology. Insolubility, reshaping, creep and relaxation properties have been studied for these new internally catalysed vitrimers.

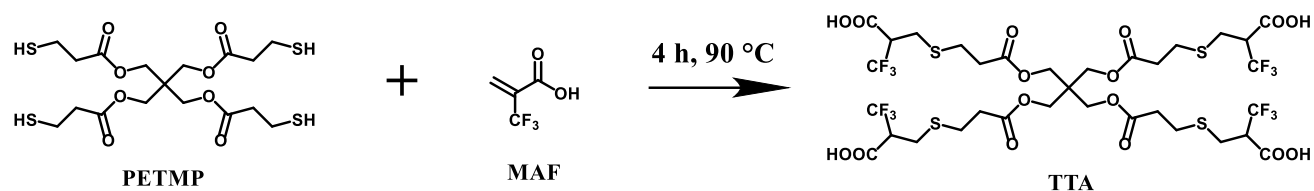
RESULTS AND DISCUSSION

Synthesis of the tetra-acid (TTA)

The thia-Michael addition has emerged as a powerful approach to build carbon-sulfur (C–S) bonds, yielding thioethers in high yields under mild reaction conditions. Numerous catalysts have been used to perform thia-Michael reactions, as recently reviewed by A. Sharma *et al.*⁴⁸ In contrast, A. Fokin *et al.*⁴⁹ performed the thia-Michael reaction under catalyst-free conditions on an activated acrylic acid. They compared the reactivity of acrylic acids activated by an α - or β -trifluoromethyl substituent with thiols and demonstrated an accelerating effect of the fluorinated group. The inductive effect of the CF₃ group was also highlighted by J. Zhao *et al.*,⁵⁰ who performed a catalyst-free thia Michael addition of aryl thiols to 3-(2,2,2-trifluoroethylidene)oxindoles.

Here, a tetra-acid (TTA) bearing CF₃ groups in the α positions of the acid functions was synthesized using the catalyst-free thia-Michael addition of pentaerythritol tetrakis(3-mercaptopropionate) (PETMP) onto 2-(trifluoromethyl)acrylic acid (MAF). The reaction was carried out at 90 °C for 4 h under solvent-free conditions (Scheme 1). The high temperature was required to maintain a low viscosity of the mixture and enable stirring. TTA was obtained as a highly viscous and transparent liquid in high yields (> 99%).

Scheme 1. Synthesis of TTA via thia-Michael addition



The FTIR spectra of the starting materials and TTA in the 1550-1850 cm^{-1} region are presented in Figure 1. The MAF FTIR spectrum is characterized by C=C (1630 cm^{-1}) and by splitted carboxylic acid C=O (1692 cm^{-1}) stretching vibrations, while the PETMP FTIR spectrum shows the characteristic absorption of the ester C=O bond at 1725 cm^{-1} . In contrast, the FTIR spectrum of the TTA product exhibits a band at 1732 cm^{-1} corresponding to the C=O of the ester functions, overlapping with the split carboxylic acid peak. Such splitting of the carboxylic acid FTIR signal (with two potential maxima around 1700 cm^{-1} and 1750 cm^{-1}) was already observed on pivalic acid.⁵¹

^1H , ^{13}C and ^{19}F NMR (Figures S1-3), as well as mass spectrometry (Figure S4) analyses confirmed the successful synthesis of TTA. The integration of the ^1H -NMR spectrum confirmed the molecular structure of TTA. The mass spectrum shows the molecular peak at $m/z = 1049$ corresponding to the proton adduct of TTA, and a peak at $m/z = 821$ corresponding to the proton adduct after scission of one ester bond.

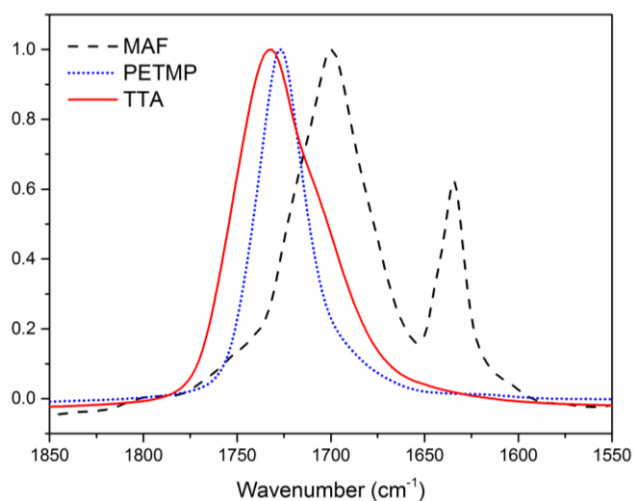


Figure 1. FTIR spectra of MAF (black dashed line), PETMP (blue dotted line) and TTA (red full line) between 1550 and 1850 cm^{-1} .

These results demonstrate that the presence of a CF_3 group in the α -position of the acid exerts an inductive activation, allowing the thia Michael addition to proceed without the use of any external catalyst, confirming the above mentioned precedent by Zhao *et al.*⁵⁰

Vitrimer synthesis

Polyester synthesis by epoxide ring-opening with carboxylic acids generally requires high temperatures as well as a catalyst.⁵² Here, we demonstrate the formation of an epoxy vitrimer network at 90 °C under catalyst-free conditions by overnight reaction of TTA with DGEBA or BDGE (Scheme 2). A transparent colorless solid (VD) was obtained from the reaction of TTA with DGEBA while a yellow transparent solid (VB) resulted from the reaction of TTA with BDGE. FTIR, DSC and rheological analyses were performed on VD to monitor the curing reaction.

The curing at 90 °C of the VD polymer network was monitored by FTIR (Figure S5). Once the polyaddition reaction between acid and epoxy groups started, the characteristic epoxide δ_{COC} absorption band⁵³ (903-926 cm^{-1}) decreased. The normalized epoxy peak intensity at different curing times is presented in Figure 3. The initial intense absorption in the 1650-1760 cm^{-1} region corresponds to the overlap of the TTA ester and acid functions already mentioned. As the reaction proceeded, the acid absorption band was expected to decrease and to be replaced by the absorption of the newly formed hydroxy ester bond in the vitrimer network. However, due to the close proximity of these bands and the splitting of the carboxylic acid band, the corresponding peaks could not be clearly distinguished.⁵⁴ The FTIR spectra of VB before and after curing (Figure S6) showed the same behaviour as those of VD.

Scheme 2. Synthesis of VD from TTA and DGEBA, and of VB from TTA and BDGE

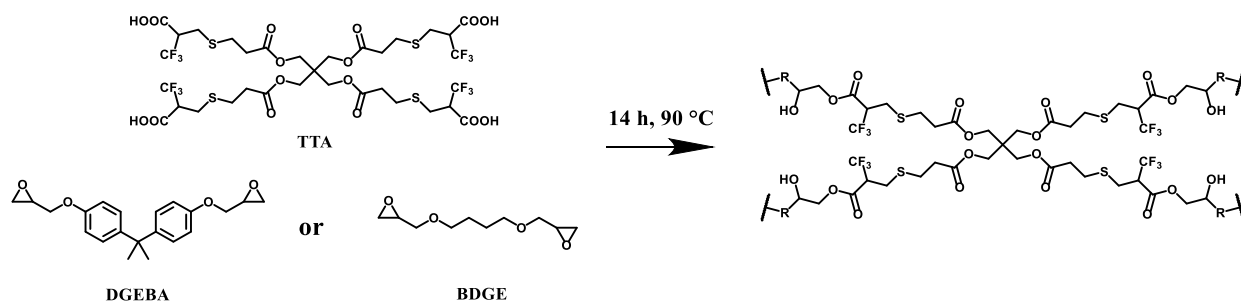


Figure 2a shows the DSC thermograms of the first heating ramp of the DGEBA/TTA mixture at different heating rates. The reaction exhibited an exothermic peak in the 30–130 °C range. By integration of the peak area, the enthalpy value was estimated at 140 J g⁻¹. This value did not vary much depending on the heating rates used, indicating complete curing under all the assessed conditions. Using Ozawa's method,⁵⁵ the activation energy E_a of the epoxy ring-opening reaction was calculated at 87 kJ mol⁻¹ for **VD** (Figure 2b). This value is close to those of other epoxy systems; for example, the reported E_a of a hexahydrophthalic anhydride-cured TGDDM epoxy (4,4'-methylenebis(*N,N*-diglycidylaniline)) and of a 4,4'-methylenedianiline-cured BPA epoxy are 74 and 129 kJ mol⁻¹, respectively.^{56,57} A similar E_a value (74 kJ mol⁻¹) was reported for catalyst-free vitrimers prepared by curing a vegetable oil-derived diacid and a tetrafunctional glycidylamine epoxy (TGDDM).⁵⁸

Isothermal DSC analyses at 90 °C were also performed on the reaction mixture of **VD** (Figure S7). An exothermic peak was observed with an enthalpy value close to the one obtained during non-isothermal DSC analyses (143 J g⁻¹ for **VD**). In addition, no residual exothermic peak was observed on the further non-isothermal DSC analyses performed after the isothermal curing at 90 °C. This confirmed the complete curing at 90 °C. Figure 3 shows the reaction progress versus time for **VD** determined by integration of the DSC exothermic peak and by integration of the epoxy absorption band from the FTIR kinetics. The DSC and FTIR data are in good agreement. The polyaddition reaction yielding **VD** seemed to be almost complete after 30 minutes at 90 °C. However, to ensure full conversion of the epoxy functions and to permit the network self-arrangement, the product was left overnight at 90 °C. A relatively high temperature is required to provide network mobility and allow reaching high conversions, due to the high viscosity.

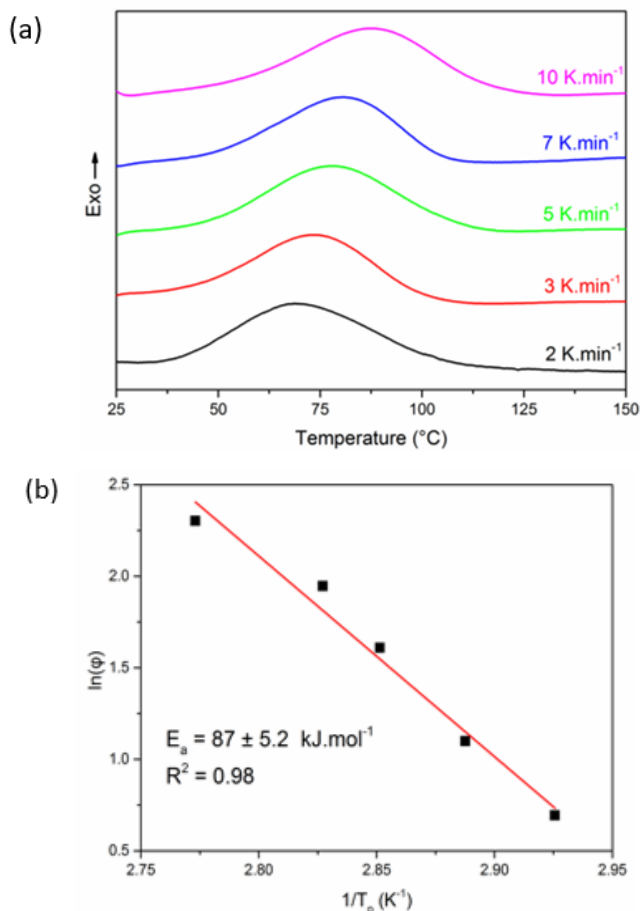


Figure 2. (a) DSC thermograms of non-isothermal curing of the DGEBA/TTA mixture with heating rate ranging from 2 to 10 K.min⁻¹. (b) Determination of the activation energy by linear fitting $1/T_p$ and $\ln(\phi)$ using Ozawa equation (Equation S1).

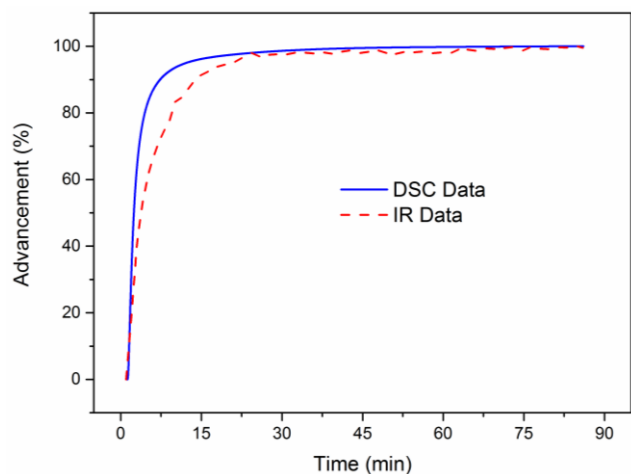


Figure 3. Reaction progress versus time for the **VD** formation at 90°C calculated from DSC (full blue curve) and FTIR (dashed red curve) data.

Rheological analyses were performed on the **VD** reaction mixture to study the network formation. First, a temperature ramp ($1\text{ }^{\circ}\text{C min}^{-1}$) analysis was carried out to determine the required curing temperature (Figure S8). The reaction seemed to start at 45 °C, which is consistent with the non-isothermal DSC analyses. The gel point was reached at 75 °C and the reaction seemed to speed up above 90 °C. The decrease of G' and G'' around 90 °C was systematically observed and is likely due to the dominance of the temperature-induced viscosity drop with respect to the expected acceleration of the crosslinking reaction in this specific temperature range.

Figure 4 shows the time evolution of the viscoelastic properties during the curing at 90 °C. The epoxy network formation occurred quickly with a transition associated with a $\tan(\delta)$ maximum after 400 s. As the reaction is particularly fast, there is a pre-reticulation of the material before the analysis, which explained why G' is already superior to G'' at the beginning of the experiment. After 15 min the system reached a stable state as the epoxy-ring opening reaction is complete.

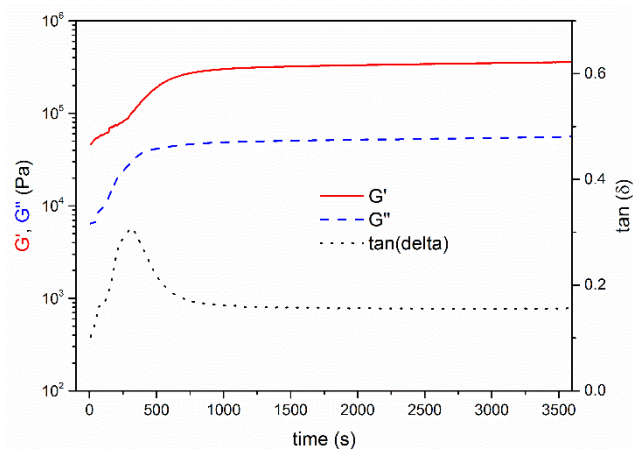


Figure 4. Evolutions of G' (full red line), G'' (dashed blue line) and $\tan(\delta)$ (dotted black line) with curing time for the **VD** formation at a curing temperature of 90 °C.

The thermal curing of **VD** has been studied in details, the observed effect of the CF_3 can be extrapolated to **VB** formation as the same curing reaction was used for both systems. This fast curing at a relatively low temperature is consistent with an activation by the $\alpha\text{-CF}_3$ group of the epoxy-acid ring opening reaction. This remarkable catalyst-free epoxide-acid ring opening is likely due to the inductive effect of the CF_3 group that decreases the pK_a of the acid, ensuring an efficient activation of the acid. Comparatively, in the absence of catalyst, non-activated acids require higher temperatures and longer times to open the epoxide rings.^{52,59}

The DSC analyses of the polymer networks obtained after curing revealed T_g values of 35 °C and -3 °C for **VD** (Figure 5) and **VB** (Figure S9), respectively. This difference is likely caused by the more rigid structure of the aromatic DGEBA compared to the aliphatic BDGE. **VD** and **VB** were not soluble after 24 h immersion in THF, which confirmed the network formation. The moderately high insoluble fraction values (>70%) may be caused by the formation of soluble oligomers during the curing process, due to transesterification reactions.⁵⁹ Finally, according to the TGA analyses, **VD** (Figure 6) and **VB** (Figure S10) were thermally stable up to 210 °C (less than 5 wt% loss).

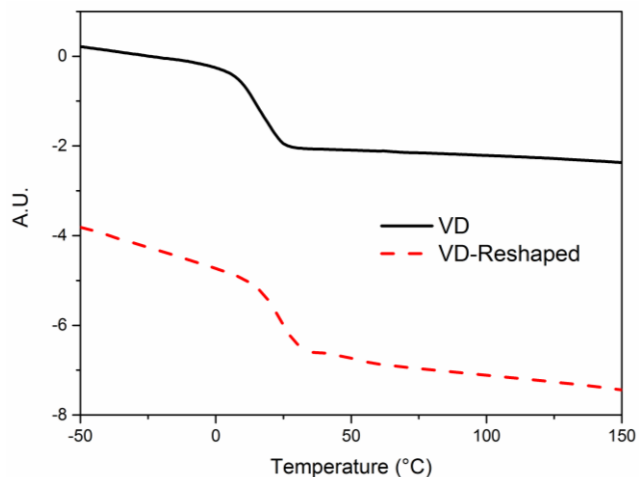


Figure 5. DSC thermograms of the second heating ramp showing the glass transition of cured (full black curve) and reshaped (dashed red curve) **VD**.

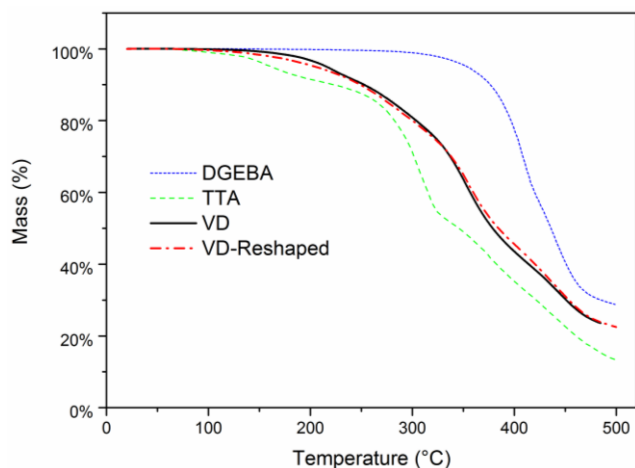


Figure 6. TGA thermograms for the monomers (DGEBA: dotted blue curve, TTA: dashed green curve) and cured (full black curve) and reshaped (dash-dot red curve) VD.

It is important to mention here that a direct comparison between CF_3 - and CH_3 -bearing analogs was not possible. Indeed the CH_3 -containing material could not be prepared because a) the thia Michael addition on methacrylic acid which would have produced the non-fluorinated equivalent of TTA did not proceed, and b) the non catalyzed epoxy-acid reaction using non-fluorinated acids requires high temperature and may lead to non-negligible side reactions.^{60,61} Indeed, high temperatures trigger dehydration and formation of ether linkages which are not exchangeable.⁶² Therefore, the resulting non-fluorinated material may not be strictly comparable to the fluorinated one. Nevertheless, the fact that the epoxy-acid reaction readily occurred at low temperature indicates that the fluorine atoms strongly affect the reactivity of the acid. This is a first hint that the strong electron-withdrawing effect of the fluorine may also affect the reactivity of the ester and promotes the transesterification, as demonstrated in the following section. In addition, as mentioned in the introduction, the polyester network prepared by Leibler et al with only 0.1 mol% of Zn catalyst does not behave as a vitrimer.³⁹

Network dynamics

The flow properties of the epoxy networks were studied by stress-relaxation and creep experiments. For the stress-relaxation tests, a 1% torsional strain was applied and the relaxation modulus ($G(t)$) was monitored as a function of time. Relaxation experiments were performed at temperatures ranging from 130 to 190 °C for VD (Figure 7a) and from 110 to 150 °C for VB (Figure 7b). The non-normalized relaxation analysis of VD and VB are respectively represented in Figure S11 and S12.

For VD, these relaxation times ranged from 10^4 s at 130 °C to 708 s at 190 °C and for VB 12800 s at 110 °C to 1400 s at 150 °C, and were similar to those of other vitrimers reported so far.³⁹ The Kohlrausch-Williams-Watts (KWW) β values were of 0.56 ± 0.02 and 0.53 ± 0.03 for VD and VB and were independent of temperature, indicating that the material flow behaviour is associated with a distribution of

relaxations rather than with a single relaxation time kinetics. The relaxation time vs. temperature data of both systems followed an Arrhenius law (Figure 8), yielding E_a values of 67 and 71 kJ mol^{-1} for VD and VB, respectively. These E_a values are close to each other as the two systems are based on the same activated transesterification reaction. Although comparing E_a values of different systems is difficult due to the influence of the polymer matrix,⁶³ the E_a determined for VD and VB are comparable to those reported for other epoxy vitrimers based on catalyzed transesterification reactions.³⁹

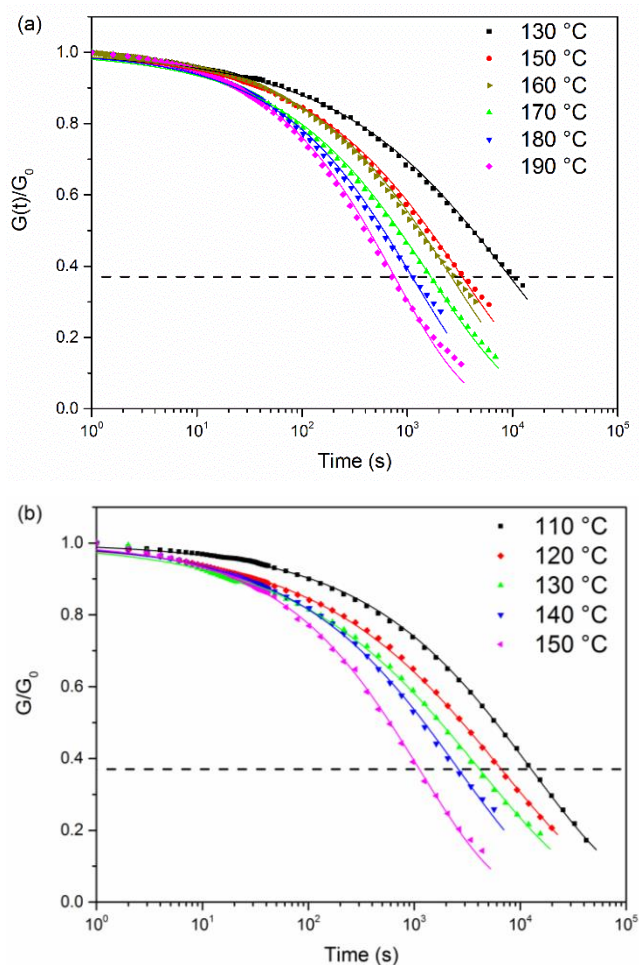


Figure 7. Normalized stress-relaxation curves (dot curves) at different temperatures for VD fitted with the Kohlrausch-Williams-Watts (KWW) model equation (dashed curves) for a 1% deformation a) for VD and b) for VB

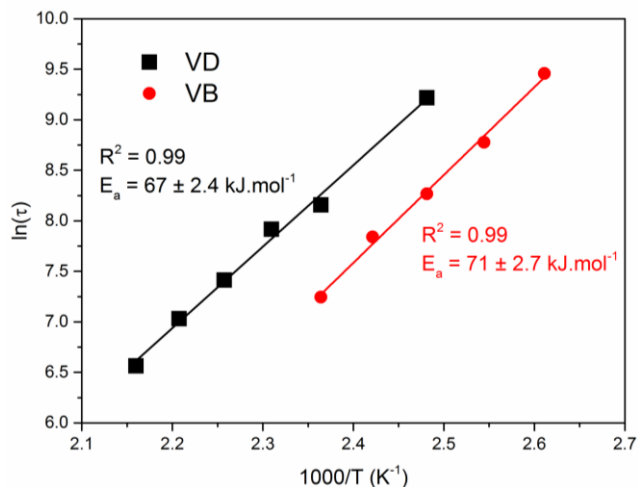


Figure 8. Fitting of the relaxation time (τ) vs. temperature data by the Arrhenius equation for **VD** (black squares) and **VB** (red circles).

Creep experiments were also performed to evaluate the flow properties of the materials. This method provides interesting results for the characterization of vitrimers with very slow dynamics and avoids the shortcoming of low force measurements.⁶⁴ Creep and recovery data at temperature ranging from 100 °C to 200 °C are presented in Figure 9a (**VD**) and Figure 9b (**VB**).

β -Hydroxy ester links are particularly well suited for transesterifications, as the proximity of the hydroxyl group will facilitate the exchange reaction.^{14,30,31} Here, the presence of a CF_3 and of an hydroxyl group on the α - and β -carbons of the ester respectively promotes the exchange reactions. The hydroxyl group probably accelerates the transesterification reaction via formation of H-bonds, while the fluorinated group renders the ester function more electrophilic thanks to its inductive effect. These combined effects dramatically increase the transesterification rates and enable the polymer network reprocessing in the absence of catalysts.

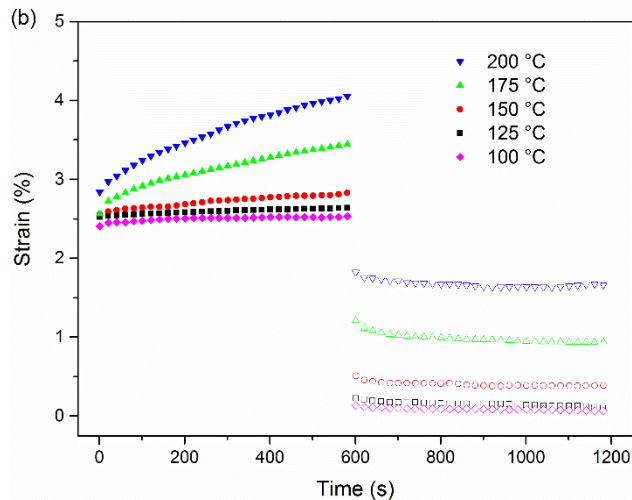
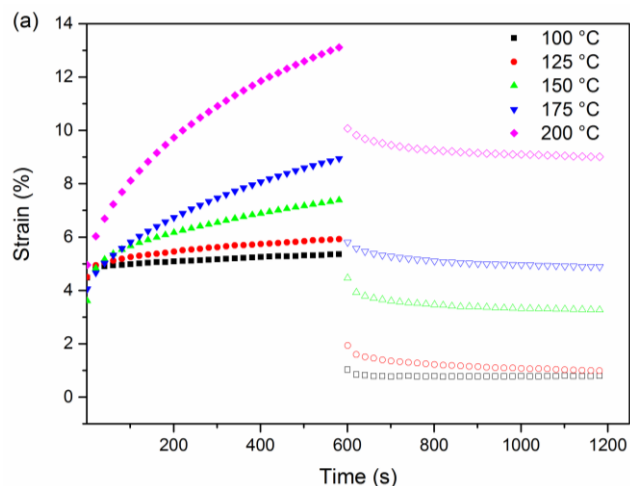


Figure 9. Creep and recovery behaviour at different temperatures for an applied stress of 10^4 Pa a) for **VD** and b) for **VB**. A steady-state is observed after 200 s during creep for each sample.

During creep-recovery analysis, the elastic deformation was observed during the initial seconds of the experiments. The initial elastic deformation appeared to be independent of the temperature and corresponded to a deformation of approximately 4-5 % and 2.5 % for **VD** and **VB** respectively. After creep, the elastic deformation was recovered. In the plastic deformation region, the compliance $J(t)$ reached a steady-state flow scaling of one at all temperatures for **VD** and **VB** after 200 s. These results confirmed the capacity of these systems to flow under stress and are in good agreement with the reshaping properties presented in the following section.

Reprocessing

VD and **VB** were cut into small pieces and submitted to the reprocessing protocol described in the experimental section (150 °C, 50 bar, 2 h). This thermal and pressure treatment resulted in the reshaping of the materials small fragments into homogeneous ribbons (Figure 10). The reshaped materials were compared to the initial vitrimers using thermo-mechanical analyses. Figure 6 shows the TGA thermograms of the cured and reshaped **VD** samples, as well as those of the monomers, from room temperature (ca. 20 °C) to 500 °C. The initial and reshaped materials feature a nearly identical mass loss profile, indicating that the reshaping process did not significantly affect the material. The same behaviour was observed for **VB** (Figure S10), further confirming that the reshaping process did not alter the thermal degradation behaviour of the network.

The chemical integrity of both **VD** and **VB** after reprocessing was also confirmed by ATR-FTIR spectroscopy (Figure S13-14). Moreover, Figure 5 and Figure S9 show that the DSC thermograms of **VD** and **VB** before and after reshaping are nearly identical and that the reshaping did not affect the T_g of the materials. Finally, the swelling indexes and gel contents of the initial and reshaped materials were evaluated by immersion in THF at 25 °C for 24 h (Table 1).

The insoluble fraction values (>70%) were not affected by the reshaping process. The difference of swelling ratios between initial and reshaped samples could be explained by a rearrangement of the network structure during the reshaping process leading to a more relaxed state. The Young's moduli of the materials before and after reshaping remained within the same order of magnitude and were similar to what was observed in other vitrimer systems.^{47,65} Moreover, the alpha transition observed by DMA was not particularly broad, confirming the formation of a homogeneous network.

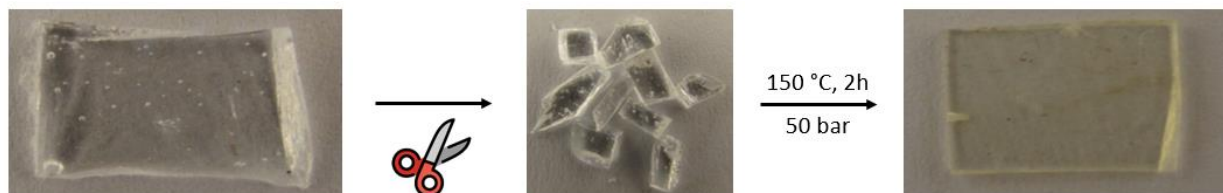


Figure 10. Visual aspect of VD before (left) and after (right) reshaping protocol. The middle picture shows the fragments of VD prior to reshaping.

Table 1. Properties of cured and reshaped vitrimer

Sample	$T_d^{5\%}$ (°C)	T_g (°C)	T_α (°C)	$E'_{-25\text{ °C}}$ (GPa)	$E'_{125\text{ °C}}$ (MPa)	Swelling index (%) ^a	Insoluble fraction (%) ^a
VD	215	35	54	3.89	2.60	358 ± 23	72 ± 2.1
VD-Reshaped	205	37	57	1.88	2.26	565 ± 13	70 ± 1.9
VB	257	-3.2	8.9	4.00	3.44	165 ± 18	78 ± 1.3
VB-Reshaped	262	-2.2	7.1	4.63	9.49	315 ± 24	78 ± 2.2

^a Test performed in THF at 25 °C for 24h.

Finally, the dynamic mechanical analyses (Figure 11 for VD and Figure S15 for VB) showed that the vitrimer storage moduli were not significantly impacted by reprocessing. The values on the rubbery plateaux before and after the reshaping process are similar. This indicates that the cross-linking density did not significantly change during the reprocessing process, as expected for an associative CAN. The T_α of VD slightly shifted to higher temperatures after reshaping while that of VB slightly decreased after reshaping. This can be correlated to network rearrangements that occurred during reshaping. In conclusion, the reshaped material retained similar mechanical properties to the initial one.

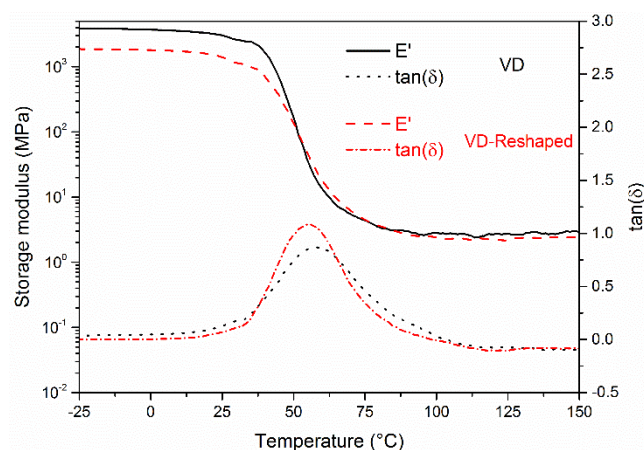


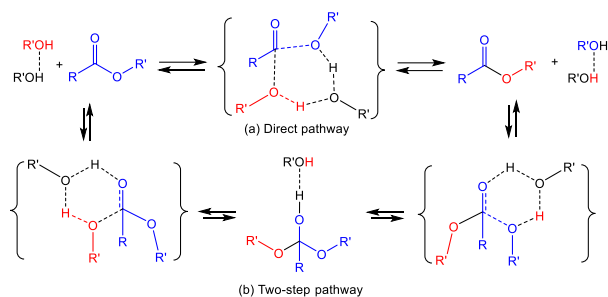
Figure 11. Storage modulus (E') and $\tan(\delta)$ of VD before (full black line and dotted black line) and after reshaping (red dashed line and red dot-dash line).

DFT investigation on a model system

In order to support the hypothesis that the electronic effect of the α -CF₃ substituent contributes to accelerate the transesterification process, DFT calculations were carried out on a model system, consisting of the degenerate transesterification of the propionate esters CX₃CH₂COOMe (X = H, F) with methanol. This model is much simpler than the ester linkages in the VB and VD vitrimers but should capture the essential electronic effect introduced by the α -CF₃ group. The effect of the β -OH group in the VB and VD materials has been previously investigated by the DFT approach for a related process, namely the amination reaction of carbonate esters,⁶⁶ which follows the same mechanism as the transesterification reaction. It was shown to originate from the OH assistance in proton relay through H-bonding. Therefore, the contribution of this substituent is not further considered here.

Transesterification can in principle follow two different pathways (see Scheme 3): a direct one with a single transition state (path a) and a two-step one with formation of a tetrahedral intermediate (path b). Both have been extensively investigated in previous computational contributions.⁶⁷⁻⁷¹ In addition, a comparative investigation of the related carbonate ester amination has concluded that both pathways occur competitively and also highlights how the barrier for each pathway is strongly affected by the number of proton relay molecules in the H-bond chain.⁷² We have opted to limit the investigation to the two step-pathway and to just one additional alcohol molecule in the H-bond chain, as illustrated in Scheme 3. Given that the tetrahedral intermediate is symmetric (the alcohol elimination of the second step is the microscopic reverse of the alcohol addition of the first step), only one transition state is of interest.

Scheme 3. Possible transesterification pathways (degenerative exchange).



The starting point of the reaction is the combination of the separate ester and MeOH dimer, $(\text{MeOH})_2$. The adduct formation from the two partners is nearly thermoneutral for both systems (Gibbs energy change, ΔG , near zero), although it is slightly more favorable for the 3,3,3-trifluoropropionate system, Figure 12. This is counterintuitive, because the most important interaction, namely the $\text{C}=\text{O}\cdots\text{H}-\text{OMe}$ H bond, should be rendered weaker by the $\alpha\text{-CF}_3$ group electron withdrawing effect. Indeed, the CF_3 system features a less negative Mulliken charge for the carbonyl O atom (-0.392 vs. -0.421 for the CH_3 system) and a longer H-bond (1.882 \AA vs. 1.814 \AA for the CH_3 system). However, the electronic energy change, ΔE , associated to the H-bond formation is essentially the same for the two systems (-12.2 and $-12.1 \text{ kcal mol}^{-1}$ for the CH_3 and CF_3 systems, respectively). Thus, the slightly more favourable ΔG for the CF_3 system must be assigned to subtle thermal and entropic effects. In these H-bonded adducts, the O atom of the attacking MeOH molecule is suitably placed for the subsequent nucleophilic addition to the carbonyl C atom.

The transition state energy for the CF_3 system is located at $21.7 \text{ kcal mol}^{-1}$ relative to the separate fragments, or $22.6 \text{ kcal mol}^{-1}$ relative to the H-bonded complex. These values are 1.3 and $0.5 \text{ kcal mol}^{-1}$ lower than those of the CH_3 system (23.0 and $23.1 \text{ kcal mol}^{-1}$), respectively. The tetrahedral intermediates are located at a relatively high energy, the CF_3 system being more stabilized by $2.8 \text{ kcal mol}^{-1}$ relative to the separate fragments (or by $1.8 \text{ kcal mol}^{-1}$ relative to the complex). The difference of reaction barrier between the CH_3 and CF_3 systems is rather small, but should definitely contribute to accelerate the transesterification reaction for the fluorinated system. From the Eyring equation, $\Delta\Delta G^\ddagger$ values of 1.3 - $0.5 \text{ kcal mol}^{-1}$ yield acceleration factors ($k_{\text{CF}_3}/k_{\text{CH}_3}$) of 9.0 - 2.3 at $25 \text{ }^\circ\text{C}$ and of 6.0 - 2.0 at $90 \text{ }^\circ\text{C}$. In comparison, the introduction of the $\beta\text{-OH}$ group was shown to lower the rate-determining barrier for the ethylene carbonate amination (i.e. ethanolamine vs. ethylamine) by $4.9 \text{ kcal mol}^{-1}$ relative to the separate reagents.⁶⁶ A comparative assistance by the $\beta\text{-OH}$ groups (not included in the model system selected for our calculations)

may also be expected for the present transesterification reaction. Thus, the calculations suggest that, although the electron-withdrawing effect of the $\alpha\text{-CF}_3$ group contributes to lower the transesterification activation barrier, this accelerating effect is probably not as important as that of a $\beta\text{-OH}$ substituent on the leaving alcohol moiety. Nevertheless, materials using only the effect of $\beta\text{-OH}$ substituent still requires the use of catalysts to be reprocessed. Here, the innovative incorporation of a $\alpha\text{-CF}_3$ group enables the transesterification to proceed without use of catalysts.

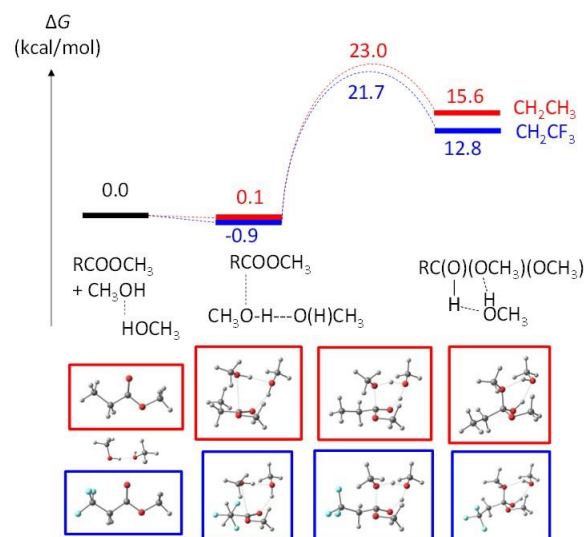


Figure 12. Gibbs energy profile (relative $G_{298\text{K},1\text{M}}$ values in kcal mol^{-1}) for the MeOH addition to $\text{CX}_3\text{CH}_2\text{COOCH}_3$ ($X = \text{H}, \text{F}$).

CONCLUSION

A new multifunctional acid (TTA) was synthesized by catalyst-free thia-Michael addition on the double bond of MAF and fully characterized. MAF proved to be a very reactive Michael acceptor thanks to the presence of a $\alpha\text{-CF}_3$ group and allowed the production of TTA in 4 h under neat conditions.

Catalyst-free vitrimers were then synthesized by the reaction of TTA with DGEBA or BDGE. Thanks to the inductive effect of the $\alpha\text{-CF}_3$ group, the curing reaction took place at $90 \text{ }^\circ\text{C}$, and was complete after one hour for the DGEBA system. The resulting products showed high thermostability and insolubility contents over 70 %, confirming the epoxy network formation. These materials were then demonstrated to be vitrimers. The stress-relaxation analyses revealed relatively fast relaxation time ($\tau = 708 \text{ s}$ at $190 \text{ }^\circ\text{C}$ for VD and $\tau = 1400 \text{ s}$ at $150 \text{ }^\circ\text{C}$ for VB). An Arrhenius behaviour was observed for materials based on DGEBA and BDGE and activation energy of 67 and 71 kJ mol^{-1} were respectively determined for these materials. Both the epoxy-acid ring opening reaction and the transesterification were vastly accelerated by the CF_3 group inductive effect in the α position of the carbonyl group. The storage modulus, the glass transitions and the insoluble fractions of the vitrimers before and after reshaping were almost identical, demonstrating that the reshaping process did not adversely affect the networks integrity.

This study demonstrates the potential of fluorinated groups as accelerating substituents for transesterification vitrimers. This original approach to catalyst-free transesterification vitrimers offers opportunities to design and prepare novel vitrimer materials based on other exchange reactions.

ASSOCIATED CONTENT

Supporting Information. Experimental details, materials, characterizations: NMR, MS, FTIR, DSC, TGA and DMA thermograms, stress relaxation and creep data.

AUTHOR INFORMATION

Corresponding Author

* Vincent Ladmiral, Vincent.Ladmiral@enscm.fr

Author Contributions

The manuscript was written through contributions of all authors. All authors have given approval to the final version of the manuscript.

Funding Sources

This work was funded by the French National Research Agency ANR (AFCAN project - ANR-19-CE06-0014) and the Institut Carnot Chimie Balard CIRIMAT (16CARN000801), and was granted access to the resources of the CICT (Centre Interuniversitaire de Calcul de Toulouse, project CALMIP).

Notes

The authors declare no competing financial interest

ABBREVIATIONS

BDGE, 1,4-butanediol diglycidyl ether; CAN, covalent adaptable network; CDCl₃, deuterated chloroform, DGEBA, bisphenol A diglycidyl ether; DFT, density functional theory; DSC, differential scanning calorimetry; E', storage modulus, E_a, activation energy; FTIR, fourier transform infrared spectroscopy; MAF, tri(fluoromethyl)acrylic acid; MS, mass spectroscopy; NGP, neighboring group participation; NMR, nuclear magnetic resonance; PETMP, pentaerythritol tetrakis(3-mercaptopropionate); T_g, glass transition temperature; TDA, 1,2,4-triazoline-3,5-dione; TGA, thermogravimetric analysis; THF, tetrahydrofuran; TTA, synthesized tetra-acid; **VB**, vitrimer obtained from BDGE; **VD**, vitrimer obtained from DGEBA

REFERENCES

- (1) Kloxin, C. J.; Bowman, C. N. Covalent Adaptable Networks: Smart, Reconfigurable and Responsive Network Systems. *Chem. Soc. Rev.* **2013**, *42*, 7161. <https://doi.org/10.1039/c3cs60046g>.
- (2) Denissen, W.; Winne, J. M.; Du Prez, F. E. Vitrimers: Permanent Organic Networks with Glass-like Fluidity. *Chem. Sci.* **2016**, *7* (1), 30–38. <https://doi.org/10.1039/C5SC02223A>.
- (3) Winne, J. M.; Leibler, L.; Du Prez, F. E. Dynamic Covalent Chemistry in Polymer Networks: A Mechanistic Perspective. *Polym. Chem.* **2019**, *10* (45), 6091–6108. <https://doi.org/10.1039/C9PY01260E>.
- (4) Lyon, G. B.; Baranek, A.; Bowman, C. N. Scaffolded Thermally Remendable Hybrid Polymer Networks. *Adv. Funct. Mater.* **2016**, *26* (9), 1477–1485. <https://doi.org/10.1002/adfm.201505368>.
- (5) Reutenauer, P.; Buhler, E.; Boul, P. J.; Candau, S. J.; Lehn, J.-M. Room Temperature Dynamic Polymers Based on Diels-Alder Chemistry. *Chem. - A Eur. J.* **2009**, *15* (8), 1893–1900. <https://doi.org/10.1002/chem.200802145>.
- (6) Chen, X.; Dam, M. A.; Ono, K.; Mal, A.; Shen, H.; Nutt, S. R.; Sheran, K.; Wudl, F. A Thermally Re-Mendable Cross-Linked Polymeric Material. *Science (80-.)*. **2002**, *295* (5560), 1698–1702. <https://doi.org/10.1126/science.1065879>.
- (7) Zhang, B.; Digby, Z. A.; Flum, J. A.; Foster, E. M.; Sparks, J. L.; Konkolewicz, D. Self-Healing, Malleable and Creep Limiting Materials Using Both Supramolecular and Reversible Covalent Linkages. *Polym. Chem.* **2015**, *6* (42), 7368–7372. <https://doi.org/10.1039/c5py01214g>.
- (8) Billiet, S.; De Bruycker, K.; Driessen, F.; Goossens, H.; Van Speybroeck, V.; Winne, J. M.; Du Prez, F. E. Triazolinediones Enable Ultrafast and Reversible Click Chemistry for the Design of Dynamic Polymer Systems. *Nat. Chem.* **2014**, *6* (9), 815–821. <https://doi.org/10.1038/nchem.2023>.
- (9) Houck, H. A.; De Bruycker, K.; Billiet, S.; Dhanis, B.; Goossens, H.; Catak, S.; Van Speybroeck, V.; Winne, J. M.; Du Prez, F. E. Design of a Thermally Controlled Sequence of Triazolinedione-Based Click and Transclick Reactions. *Chem. Sci.* **2017**, *8* (4), 3098–3108. <https://doi.org/10.1039/c7sc00199c>.
- (10) Kuhl, N.; Geitner, R.; Bose, R. K.; Bode, S.; Dietzek, B.; Schmitt, M.; Popp, J.; Garcia, S. J.; van der Zwaag, S.; Schubert, U. S.; Hager, M. D. Self-Healing Polymer Networks Based on Reversible Michael Addition Reactions. *Macromol. Chem. Phys.* **2016**, *217* (22), 2541–2550. <https://doi.org/10.1002/macp.201600353>.
- (11) Zhang, B.; Digby, Z. A.; Flum, J. A.; Chakma, P.; Saul, J. M.; Sparks, J. L.; Konkolewicz, D. Dynamic Thiol-Michael Chemistry for Thermoresponsive Rehealable and Malleable Networks. *Macromolecules* **2016**, *49* (18), 6871–6878. <https://doi.org/10.1021/acs.macromol.6b01061>.
- (12) Liu, W. X.; Zhang, C.; Zhang, H.; Zhao, N.; Yu, Z. X.; Xu, J. Oxime-Based and Catalyst-Free Dynamic Covalent Polyurethanes. *J. Am. Chem. Soc.* **2017**, *139* (25), 8678–8684. <https://doi.org/10.1021/jacs.7b03967>.
- (13) Jin, K.; Li, L.; Torkelson, J. M. Recyclable Crosslinked Polymer Networks via One-Step Controlled Radical Polymerization. *Adv. Mater.* **2016**, *28* (31), 6746–6750. <https://doi.org/10.1002/adma.201600871>.
- (14) Montarnal, D.; Capelot, M.; Tournilhac, F.; Leibler, L. Silica-Like Malleable Materials from Permanent Organic Networks. *Science (80-.)*. **2011**, *334*, 965–968. <https://doi.org/10.1126/science.1212648>.
- (15) Denissen, W.; Rivero, G.; Nicolay, R.; Leibler, L.; Winne, J. M.; Du Prez, F. E. Vinyllogous Urethane Vitrimers. *Adv. Funct. Mater.* **2015**, *25* (16), 2451–2457. <https://doi.org/10.1002/adfm.201404553>.
- (16) Spiesschaert, Y.; Taplan, C.; Stricker, L.; Guerre, M.; Winne, J. M.; Du Prez, F. E. Influence of the Polymer Matrix on the Viscoelastic Behaviour of Vitrimers. *Polym. Chem.* **2020**, *11* (33), 5377–5385. <https://doi.org/10.1039/d0py00144g>.
- (17) Fortman, D. J.; Brutman, J. P.; Cramer, C. J.; Hillmyer, M. A.; Dichtel, W. R. Mechanically Activated, Catalyst-Free Polyhydroxyurethane Vitrimers. *J. Am. Chem. Soc.* **2015**, *137* (44), 14019–14022. <https://doi.org/10.1021/jacs.5b08084>.
- (18) Chao, A.; Negulescu, I.; Zhang, D. Dynamic Covalent Polymer Networks Based on Degenerative Imine Bond Exchange: Tuning the Malleability and Self-Healing Properties by Solvent. *Macromolecules* **2016**, *49* (17), 6277–6284. <https://doi.org/10.1021/acs.macromol.6b01443>.
- (19) Obadia, M. M.; Mudraboyina, B. P.; Serghei, A.; Montarnal, D.; Drockenmuller, E. Reprocessing and Recycling of Highly Cross-Linked Ion-Conducting Networks through Transalkylation Exchanges of C-N Bonds. *J. Am. Chem. Soc.* **2015**, *137* (18), 6078–6083. <https://doi.org/10.1021/jacs.5b02653>.
- (20) Li, Q.; Ma, S.; Wang, S.; Yuan, W.; Xu, X.; Wang, B.; Huang, K.; Zhu, J. Facile Catalyst-Free Synthesis, Exchanging, and Hydrolysis of an Acetal Motif for Dynamic Covalent Networks. *J. Mater. Chem. A* **2019**, *7* (30), 18039–18049.

- <https://doi.org/10.1039/C9TA04073K>.
- (21) Röttger, M.; Domenech, T.; Van Der Weegen, R.; Breuillac, A.; Nicolaÿ, R.; Leibler, L. High-Performance Vitrimers from Commodity Thermoplastics through Dioxaborolane Metathesis. *Science* (80-.). **2017**, *356* (6333), 62–65. <https://doi.org/10.1126/science.aah5281>.
- (22) Lijsebetten, F. Van; Spiesschaert, Y.; Winne, J. M.; Prez, F. E. Du. Reprocessing of Covalent Adaptable Polyamide Networks through Internal Catalysis and Ring-Size Effects. *J. Am. Chem. Soc.* **2021**, *jacs.1c07360*. <https://doi.org/10.1021/JACS.1C07360>.
- (23) Boucher, D.; Madsen, J.; Caussé, N.; Pébère, N.; Ladmiral, V.; Negrell, C. Hemiacetal Ester Exchanges, Study of Reaction Conditions and Mechanistic Pathway. *React. 2020, Vol. 1, Pages 89-101* **2020**, *1* (2), 89–101. <https://doi.org/10.3390/REACTIONS1020008>.
- (24) Boucher, D.; Madsen, J.; Yu, L.; Huang, Q.; Caussé, N.; Pébère, N.; Ladmiral, V.; Negrell, C. Polystyrene Hybrid-Vitrimer Based on the Hemiacetal Ester Exchange Reaction. *Macromolecules* **2021**, *54* (14), 6772–6779. <https://doi.org/10.1021/ACS.MACROMOL.1C00948>.
- (25) Altuna, F. I.; Casado, U.; Dell'Erba, I. E.; Luna, L.; Hoppe, C. E.; Williams, R. J. J. Epoxy Vitrimers Incorporating Physical Crosslinks Produced by Self-Association of Alkyl Chains. *Polymer Chemistry*. **2020**, pp 1337–1347. <https://doi.org/10.1039/c9py01787a>.
- (26) Altuna, F. I.; Hoppe, C. E.; Williams, R. J. J. Shape Memory Epoxy Vitrimers Based on DGEBA Crosslinked with Dicarboxylic Acids and Their Blends with Citric Acid. *RSC Adv.* **2016**, *6* (91), 88647–88655. <https://doi.org/10.1039/c6ra18010h>.
- (27) Hayashi, M.; Yano, R.; Takasu, A. Synthesis of Amorphous Low Tg Polyesters with Multiple COOH Side Groups and Their Utilization for Elastomeric Vitrimers Based on Post-Polymerization Cross-Linking. *Polym. Chem* **2019**, *10*, 2047. <https://doi.org/10.1039/c9py00293f>.
- (28) Sastri, V. R.; Tesoro, G. C. Reversible Crosslinking in Epoxy Resins. II. New Approaches. *J. Appl. Polym. Sci.* **1990**, *39* (7), 1439–1457. <https://doi.org/10.1002/app.1990.070390703>.
- (29) Pascualt, J. P.; Williams, R. J. J. *Epoxy Polymers: New Materials and Innovations*; **2010**. <https://doi.org/10.1002/9783527628704>.
- (30) Capelot, M.; Montarnal, D.; Tournilhac, F.; Leibler, L. Metal-Catalyzed Transesterification for Healing and Assembling of Thermosets. *J. Am. Chem. Soc.* **2012**, *134* (18), 7664–7667. <https://doi.org/10.1021/ja302894k>.
- (31) Capelot, M.; Unterlass, M. M.; Tournilhac, F.; Leibler, L. Catalytic Control of the Vitrimer Glass Transition. *ACS Macro Lett.* **2012**, *1* (7), 789–792. <https://doi.org/10.1021/mz300239f>.
- (32) Yu, K.; Taynton, P.; Zhang, W.; Dunn, M. L.; Qi, H. J. Reprocessing and Recycling of Thermosetting Polymers Based on Bond Exchange Reactions. *RSC Adv.* **2014**, *4* (20), 10108–10117. <https://doi.org/10.1039/c3ra47438k>.
- (33) Brutman, J. P.; Delgado, P. A.; Hillmyer, M. A. Polylactide Vitrimers. *ACS Macro Lett.* **2014**, *3* (7), 607–610. <https://doi.org/10.1021/mz500269w>.
- (34) Yang, Z.; Wang, Q.; Wang, T. Dual-Triggered and Thermally Reconfigurable Shape Memory Graphene-Vitrimer Composites. *ACS Appl. Mater. Interfaces* **2016**, *8*, 37. <https://doi.org/10.1021/acsami.6b07403>.
- (35) Liu, T.; Zhao, B.; Zhang, J. Recent Development of Repairable, Malleable and Recyclable Thermosetting Polymers through Dynamic Transesterification. *Polymer (Guildf)*. **2020**, *194*, 122392. <https://doi.org/10.1016/j.polymer.2020.122392>.
- (36) Yang, X.; Guo, L.; Xu, X.; Shang, S.; Liu, H. A Fully Bio-Based Epoxy Vitrimer: Self-Healing, Triple-Shape Memory and Reprocessing Triggered by Dynamic Covalent Bond Exchange. *Mater. Des.* **2020**, *186*, 108248. <https://doi.org/10.1016/j.matdes.2019.108248>.
- (37) Van Zee, N. J.; Nicolaÿ, R. Vitrimers: Permanently Crosslinked Polymers with Dynamic Network Topology. *Prog. Polym. Sci.* **2020**, *104*, 101233. <https://doi.org/10.1016/j.progpolymsci.2020.101233>.
- (38) Guerre, M.; Taplan, C.; Winne, J. M.; Du Prez, F. E. Vitrimers: Directing Chemical Reactivity to Control Material Properties. *Chem. Sci.* **2020**, *11* (19), 4855–4870. <https://doi.org/10.1039/DoSC01069C>.
- (39) Cuminet, F.; Caillol, S.; Dantras, É.; Leclerc, É.; Ladmiral, V. Neighboring Group Participation and Internal Catalysis Effects on Exchangeable Covalent Bonds: Application to the Thriving Field of Vitrimer Chemistry. *Macromolecules* **2021**, *54* (9), 3927–3961. <https://doi.org/10.1021/acs.macromol.0c02706>.
- (40) Han, J.; Liu, T.; Hao, C.; Zhang, S.; Guo, B.; Zhang, J. A Catalyst-Free Epoxy Vitrimer System Based on Multifunctional Hyperbranched Polymer. *Macromolecules* **2018**, *51* (17), 6789–6799. <https://doi.org/10.1021/acs.macromol.8b01424>.
- (41) Liu, T.; Zhang, S.; Hao, C.; Verdi, C.; Liu, W.; Liu, H.; Zhang, J. Glycerol Induced Catalyst-Free Curing of Epoxy and Vitrimer Preparation. *Macromol. Rapid Commun.* **2019**, *40* (7), 1800889. <https://doi.org/10.1002/marc.201800889>.
- (42) Altuna, F. I.; Pettarin, V.; Williams, R. J. J. Self-Healable Polymer Networks Based on the Cross-Linking of Epoxidised Soybean Oil by an Aqueous Citric Acid Solution. *Green Chem.* **2013**, *15* (12), 3360–3366. <https://doi.org/10.1039/c3gc41384e>.
- (43) Delahaye, M.; Winne, J. M.; Du Prez, F. E. Internal Catalysis in Covalent Adaptable Networks: Phthalate Monoester Transesterification As a Versatile Dynamic Cross-Linking Chemistry. *J. Am. Chem. Soc.* **2019**, *141* (38), 15277–15287. <https://doi.org/10.1021/jacs.9b07269>.
- (44) Altuna, F. I.; Hoppe, C. E.; Williams, R. J. J. Epoxy Vitrimers with a Covalently Bonded Tertiary Amine as Catalyst of the Transesterification Reaction. *Eur. Polym. J.* **2019**, *113*, 297–304. <https://doi.org/10.1016/j.eurpolymj.2019.01.045>.
- (45) Nishimura, Y.; Chung, J.; Muradyan, H.; Guan, Z. Silyl Ether as a Robust and Thermally Stable Dynamic Covalent Motif for Malleable Polymer Design. *J. Am. Chem. Soc.* **2017**, *139* (42), 14881–14884. <https://doi.org/10.1021/jacs.7b08826>.
- (46) Zhang, H.; Majumdar, S.; Van Benthem, R. A. T. M.; Sijbesma, R. P.; Heuts, J. P. A. Intramolecularly Catalyzed Dynamic Polyester Networks Using Neighboring Carboxylic and Sulfonic Acid Groups. *ACS Macro Lett.* **2020**, *12*, 272–277. <https://doi.org/10.1021/acsmacrolett.9b01023>.
- (47) Debnath, S.; Kaushal, S.; Ojha, U. Catalyst-Free Partially Bio-Based Polyester Vitrimers. *ACS Appl. Polym. Mater.* **2020**, *2* (2), 1006–1013. <https://doi.org/10.1021/acsapm.0c00016>.
- (48) Wadhwa, P.; Kharbanda, A.; Sharma, A. Thia-Michael Addition: An Emerging Strategy in Organic Synthesis. *Asian J. Org. Chem.* **2018**, *7* (4), 634–661. <https://doi.org/10.1002/AJOC.201700609>.
- (49) Vasil'eva, T. P.; Kolomiets, A. F.; Mysov, E. I.; Fokin, A. V. Comparison of α - and β -Trifluoromethylsubstituted Acrylic Acids in Their Reactions with Thiols. *Russ. Chem. Bull.* **1997**, *46* (6), 1181–1183. <https://doi.org/10.1007/BF02496227>.
- (50) Chen, B.; Lei, J.; Zhao, J. Michael Addition of Aryl Thiols to 3-(2,2,2-Trifluoroethylidene)Oxindoles under Catalyst-Free Conditions: The Rapid Synthesis of Sulfur-Containing Oxindole Derivatives. *J. Chem. Res.* **2018**, *42* (4), 210–214. <https://doi.org/10.3184/174751918X15240724383170>.
- (51) Cazares-Cortes, E.; Baker, B. C.; Nishimori, K.; Ouchi, M.; Tournilhac, F. Polymethacrylic Acid Shows Thermoresponsivity in an Organic Solvent. *Macromolecules* **2019**, *52* (15), 5995–6004. <https://doi.org/10.1021/acs.macromol.9b00412>.
- (52) Blank, W. J.; He, Z. A.; Picci, M. Catalysis of the Epoxy-Carboxyl Reaction. *J. Coatings Technol.* **2002**, *74* (3), 33–41. <https://doi.org/10.1007/BF02720158>.
- (53) González, M. G.; Cabanelas, J. C.; Baselga, J. Applications of

- FTIR on Epoxy Resins - Identification, Monitoring the Curing Process, Phase Separation and Water Uptake. In *Infrared Spectroscopy - Materials Science, Engineering and Technology*; InTech, 2012; Vol. 16, p 208. <https://doi.org/10.5772/36323>.
- (54) Poutrel, Q.-A.; Blaker, J. J.; Soutis, C.; Tournilhac, F.; Gresil, M. Dicarboxylic Acid-Epoxy Vitrimers: Influence of the off-Stoichiometric Acid Content on Cure Reactions and Thermo-Mechanical Properties. *Polym. Chem.* **2020**, *11* (33), 5327–5338. <https://doi.org/10.1039/DoPY00342E>.
- (55) Ozawa, T. A New Method of Analyzing Thermogravimetric Data. *Bull. Chem. Soc. Jpn.* **1965**, *38* (11), 1881–1886. <https://doi.org/10.1246/bcsj.38.1881>.
- (56) Herman Teo, J. K.; Teo, K. C.; Pan, B.; Xiao, Y.; Lu, X. Epoxy/Polyhedral Oligomeric Silsesquioxane (POSS) Hybrid Networks Cured with an Anhydride: Cure Kinetics and Thermal Properties. *Polymer (Guildf)*. **2007**, *48* (19), 5671–5680. <https://doi.org/10.1016/j.polymer.2007.07.059>.
- (57) Lee, J. Y.; Shim, M. J.; Kim, S. W. Thermal Decomposition Kinetics of an Epoxy Resin with Rubber-Modified Curing Agent. *J. Appl. Polym. Sci.* **2001**, *81* (2), 479–485. <https://doi.org/10.1002/app.1460>.
- (58) Li, Y.; Liu, T.; Zhang, S.; Shao, L.; Fei, M.; Yu, H.; Zhang, J. Catalyst-Free Vitriimer Elastomers Based on a Dimer Acid: Robust Mechanical Performance, Adaptability and Hydrothermal Recyclability. *Green Chem.* **2020**, *22* (3), 870–881. <https://doi.org/10.1039/c9gc04080c>.
- (59) Vidil, T.; Tournilhac, F.; Musso, S.; Robisson, A.; Leibler, L. Control of Reactions and Network Structures of Epoxy Thermosets. *Prog. Polym. Sci.* **2016**, *62*, 126–179. <https://doi.org/10.1016/j.progpolymsci.2016.06.003>.
- (60) Matgijka, L.; Pokornj, S.; Dusek, K. Acid Curing of Epoxy Resins. A Comparison between the Polymerization of Diepoxide-Diacid and Monoepoxide-Cyclic Anhydride Systems. *Makromol. Chem* **1985**, *186*, 2025–2036.
- (61) Morancho, J. M.; Ramis, X.; Fernández-Francos, X.; Konuray, O.; Salla, J. M.; Serra, À. Dual Curing of an Epoxy Resin with Dicarboxylic Acids. *J. Therm. Anal. Calorim.* **2020**, *142* (2), 607–615. <https://doi.org/10.1007/s10973-020-09523-z>.
- (62) Madec, P.-J.; Maréchal, E. Kinetics and Mechanisms of Polyesterifications II. Reactions of Diacids with Diepoxides. **1985**, 153–228. https://doi.org/10.1007/3-540-15482-5_9.
- (63) Spiesschaert, Y.; Taplan, C.; Stricker, L.; Guerre, M.; Winne, J. M.; Du Prez, F. E. Influence of the Polymer Matrix on the Viscoelastic Behaviour of Vitrimers. *Polym. Chem.* **2020**, *11* (33), 5377–5385. <https://doi.org/10.1039/d0py00114g>.
- (64) Ricarte, R. G.; Tournilhac, F.; Cloître, M.; Leibler, L. Linear Viscoelasticity and Flow of Self-Assembled Vitrimers: The Case of a Polyethylene/Dioxaborolane System. *Macromolecules* **2020**, *53* (5), 1852–1866. <https://doi.org/10.1021/acs.macromol.9b02415>.
- (65) Lessard, J. J.; Garcia, L. F.; Easterling, C. P.; Sims, M. B.; Bentz, K. C.; Arencibia, S.; Savin, D. A.; Sumerlin, B. S. Catalyst-Free Vitrimers from Vinyl Polymers. *Macromolecules* **2019**, *52* (5), 2105–2111. <https://doi.org/10.1021/acs.macromol.8b02477>.
- (66) Quienne, B.; Poli, R.; Pinaud, J.; Caillol, S. Enhanced Aminolysis of Cyclic Carbonates by β -Hydroxylamines for the Production of Fully Biobased Polyhydroxyurethanes. *Green Chem.* **2021**, *23* (4), 1678–1690. <https://doi.org/10.1039/DoGC04120C>.
- (67) Horn, H. W.; Jones, G. O.; Wei, D. S.; Fukushima, K.; Lecuyer, J. M.; Coady, D. J.; Hedrick, J. L.; Rice, J. E. Mechanisms of Organocatalytic Amidation and Trans-Esterification of Aromatic Esters As a Model for the Depolymerization of Poly(Ethylene) Terephthalate. *J. Phys. Chem. A* **2012**, *116* (51), 12389–12398. <https://doi.org/10.1021/JP304212Y>.
- (68) Li, K.; Yang, Z.; Zhao, J.; Lei, J.; Jia, X.; Mushrif, S. H.; Yang, Y. Mechanistic and Kinetic Studies on Biodiesel Production Catalyzed by an Efficient Pyridinium Based Ionic Liquid. *Green Chem.* **2015**, *17* (8), 4271–4280. <https://doi.org/10.1039/C5GC00976F>.
- (69) Kaixin Li; YiBo Yan; Jun Zhao; Junxi Lei; Xinli Jia; H. Mushrif, S.; Yanhui Yang. Understanding the Role of Hydrogen Bonding in Bronsted Acidic Ionic Liquid-Catalyzed Transesterification: A Combined Theoretical and Experimental Investigation. *Phys. Chem. Chem. Phys.* **2016**, *18* (48), 32723–32734. <https://doi.org/10.1039/C6CP06502C>.
- (70) Ng, J. Q.; Arima, H.; Mochizuki, T.; Toh, K.; Matsui, K.; Ratanasak, M.; Hasegawa, J.-Y.; Hatano, M.; Ishihara, K. Chemoselective Transesterification of Methyl (Meth)Acrylates Catalyzed by Sodium(I) or Magnesium(II) Aryloxides. *ACS Catal.* **2020**, *10* (1), 199–207. <https://doi.org/10.1021/ACSCATAL.0c04217>.
- (71) Bhusal, S.; Oh, C.; Kang, Y.; Varshney, V.; Ren, Y.; Nepal, D.; Roy, A.; Kedziora, G. Transesterification in Vitriimer Polymers Using Bifunctional Catalysts: Modeled with Solution-Phase Experimental Rates and Theoretical Analysis of Efficiency and Mechanisms. *J. Phys. Chem. B* **2021**, *125* (9), 2411–2424. <https://doi.org/10.1021/acs.jpcc.0c10403>.
- (72) Zabalov, M. V.; Tiger, R. P. Specificities of Application of the Supermolecule Method to the Calculation of Reaction Mechanisms in a Protonodonor Medium. Ethylene Carbonate Aminolysis in Methanol. *Theor. Chem. Accounts* **2017**, *136* (9), 1–20. <https://doi.org/10.1007/S00214-017-2124-9>.